Journal of Geophysical Research Atmospheres

Supporting Information for

WWLLN lightning and satellite microwave radiometrics at 37 to 183 GHz: thunderstorms in the broad tropics

N. N. Solorzano[1], J. N. Thomas[2,3,4], M. L. Hutchins[4] and R. H. Holzworth[4]

[1]*Dept. of Physics, DigiPen Institute of Technology, Redmond, WA*
[2]*NorthWest Research Associates, Redmond, WA*
[3]*Dept. of Electrical and Computer Engineering, DigiPen Institute of Technology, Redmond, WA*
[4]*Dept. of Earth and Space Sciences, University of Washington, Seattle, WA*

Contents of this file

Figures S1 to S9.

Introduction

Here we show figures that address points related to relative detection efficiency, sample size, and brightness temperature reconstruction using lightning rates.

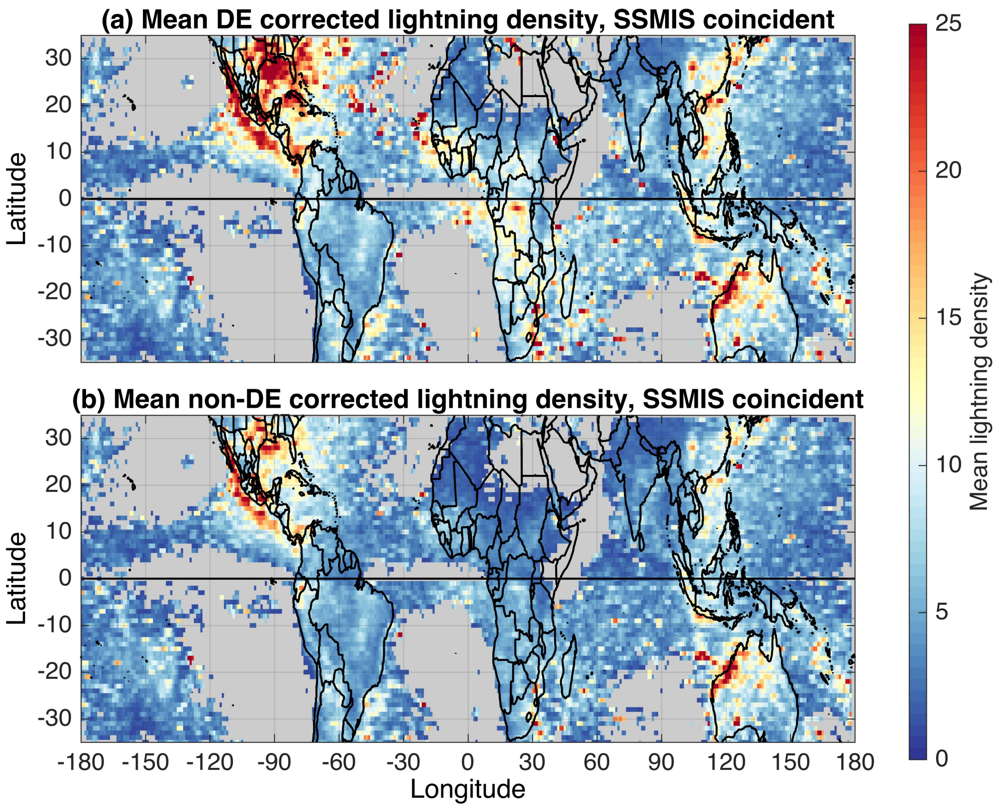

Figure S1. DE and non-DE corrected mean WWLLN lightning density per 0.5° × 0.5° grid squares and within ± 15 min of SSMIS 91.7 GHz PCT brightness temperature measurements below 250 K. These are the gridded data for two northern and southern hemisphere summers that are combined into a summer database, namely Jul., Aug., and Sep. (JAS) of 2009 and 2010 for 0°-35° N and Jan., Feb., and Mar. (JFM) of 2010 and 2011 for 0°- 35° S (see Section 2 of paper). Note that the SSMIS sensor is on the DMSP F16 satellite that passes each location on earth two times per day at about 19:00 and 07:00 LST.

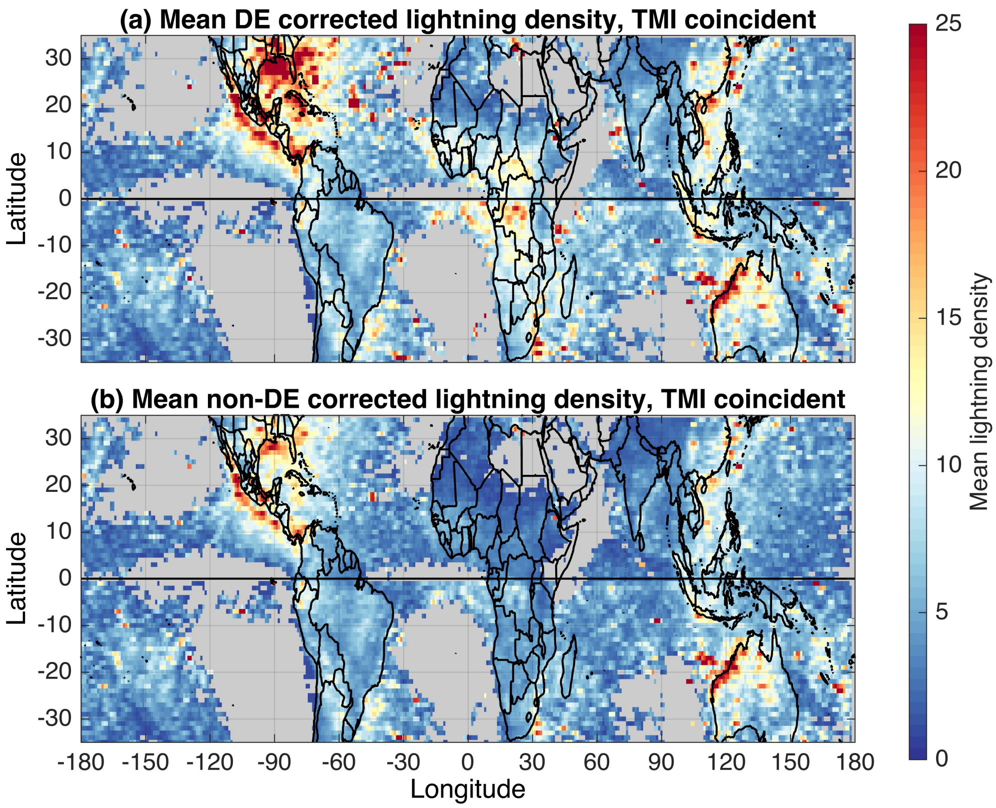

Figure S2. DE and non-DE corrected mean WWLLN lightning density per 0.5° × 0.5° grid squares and within ± 15 min of TMI 85 GHz PCT brightness temperature measurements below 250 K. These are the gridded data for two northern and southern hemisphere summers that are combined into a summer database, namely Jul., Aug., and Sep. (JAS) of 2009 and 2010 for 0°-35° N and Jan., Feb., and Mar. (JFM) of 2010 and 2011 for 0°- 35° S (see Section 2 of paper). Note that the TMI sensor on the TRMM satellite observes thunderstorms at various LSTs.

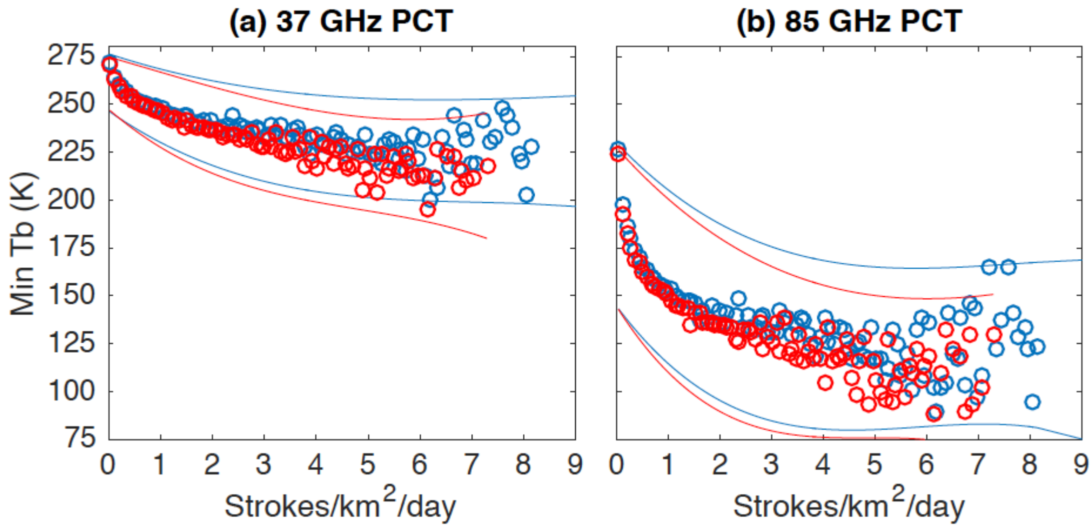

Figure S3. Scatter plot of TMI 37 (a) and 85 (b) GHz PCT minimum brightness temperatures (Tbs) and WWLLN stroke rates to compare DE corrected and non-DE corrected data. DE corrected lightning data are in blue (same as Figure 2 in paper) and non-DE corrected lightning data are in red.

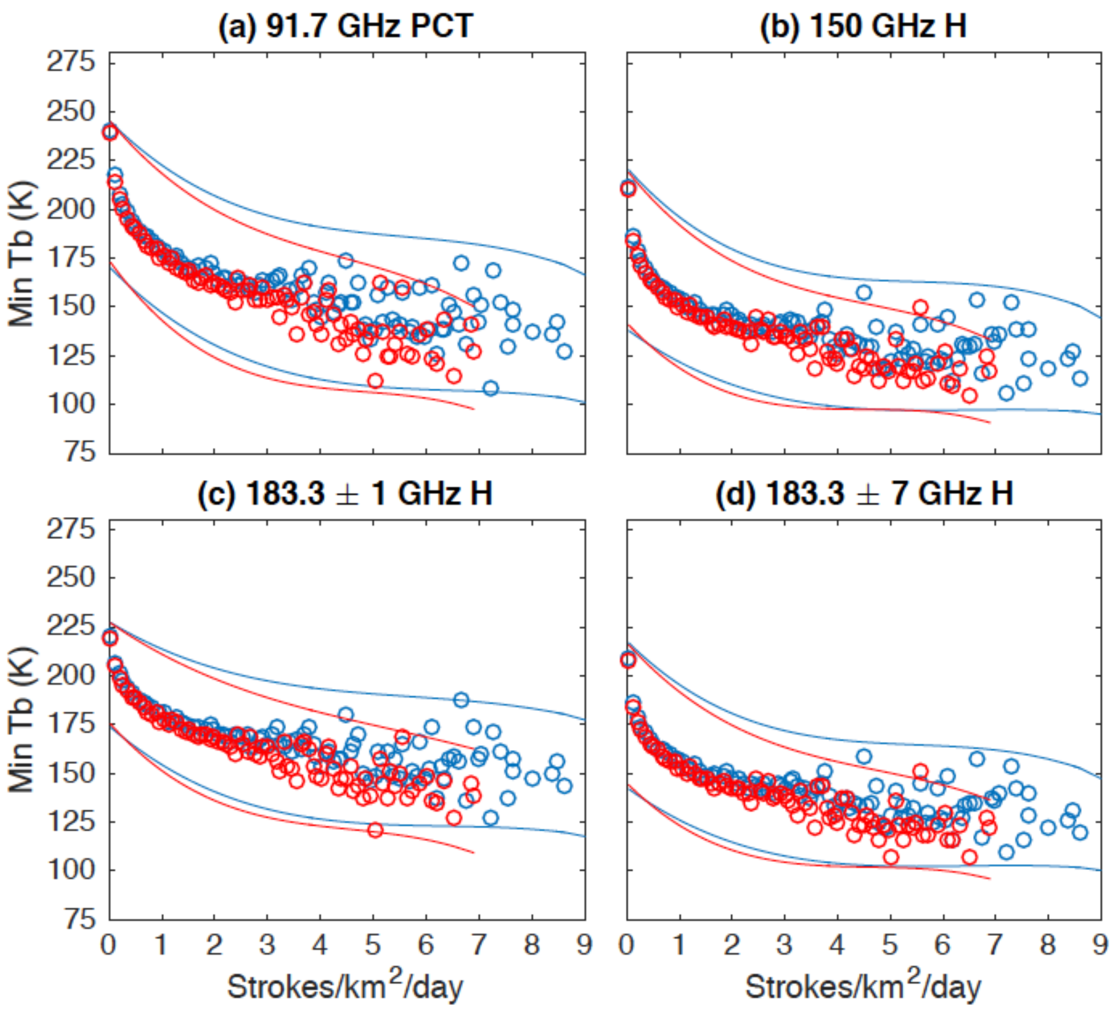

Figure S4. SSMIS/F16 91 GHz PCT (a), 150 (b), 183.3 ±1 (c), and 183.3 ±7 GHz H (d) minimum brightness temperatures and WWLLN stroke rates to compare DE corrected and non-DE corrected data. DE corrected lightning data are in blue (same a Figure 4 in paper) and non-DE corrected lightning data are in red (same as Figure 6 in paper).

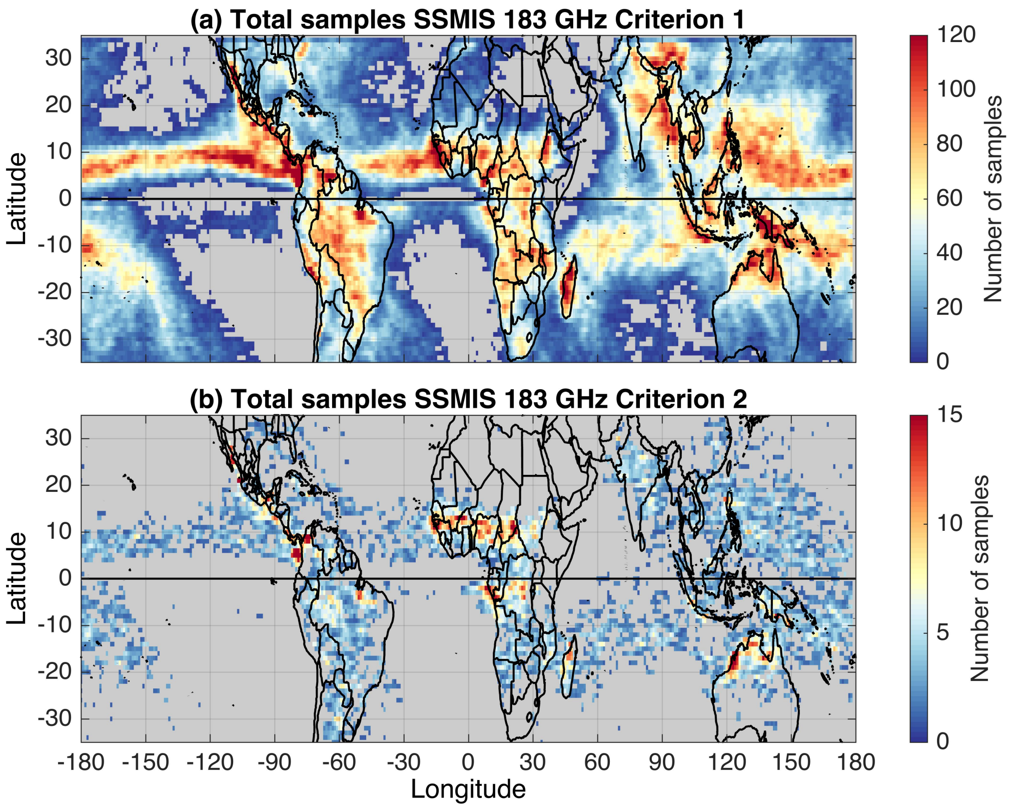

Figure S5. Total number of 0.5° × 0.5° grid square samples that satisfied the SSMIS 183 GHz criteria 1 (a) and 2 (b) with and without lightning occurrence. These data are used in the calculation of lightning probability in Figure 7. These are the gridded data for two northern and southern hemisphere summers that are combined into a summer database, namely Jul., Aug., and Sep. (JAS) of 2009 and 2010 for 0°-35° N and Jan., Feb., and Mar. (JFM) of 2010 and 2011 for 0°- 35° S (see Section 2 of paper). Note that the SSMIS sensor is on the DMSP F16 satellite that passes each location on earth two times per day at about 19:00 and 07:00 LST.

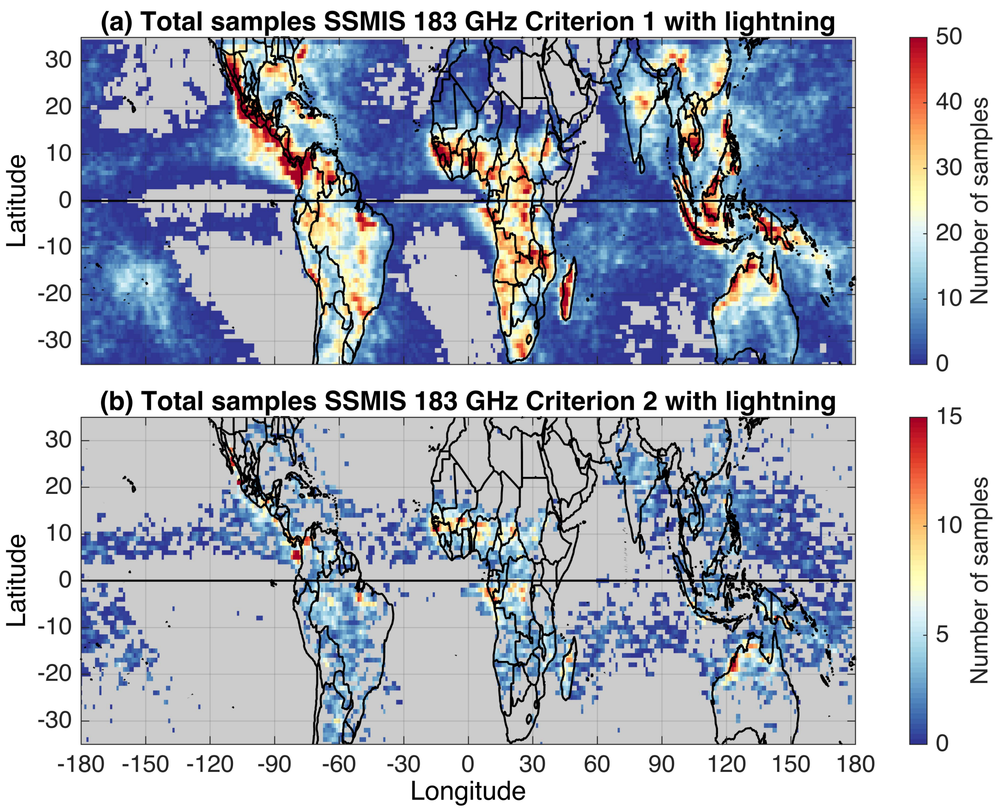

Figure S6. Total number of 0.5° × 0.5° grid square samples that satisfied the SSMIS 183 GHz criteria 1 (a) and 2 (b) with at least one lightning stroke. These data are used in the calculation of lightning probability in Figure 7. These are the gridded data for two northern and southern hemisphere summers that are combined into a summer database, namely Jul., Aug., and Sep. (JAS) of 2009 and 2010 for 0°-35° N and Jan., Feb., and Mar. (JFM) of 2010 and 2011 for 0°- 35° S (see Section 2 of paper). Note that the SSMIS sensor is on the DMSP F16 satellite that passes each location on earth two times per day at about 19:00 and 07:00 LST.

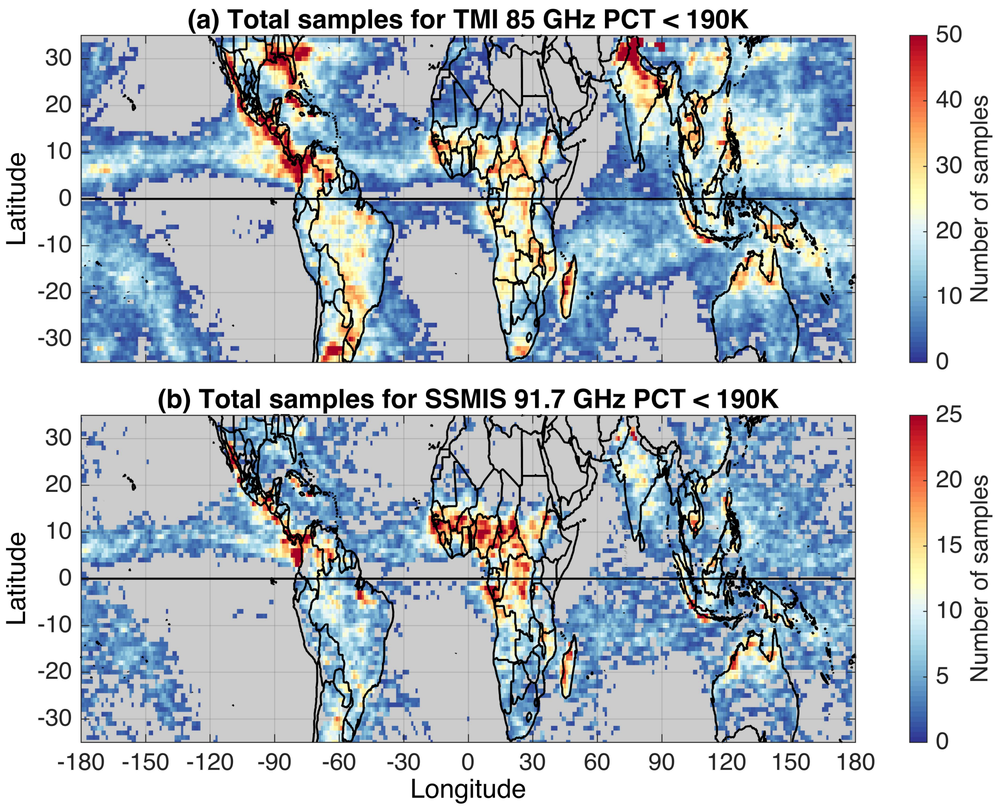

Figure S7. Total number of 0.5° × 0.5° grid square samples that satisfied TMI 85 GHz PCT < 190 K (a) and SSMIS 91.7 GHz < 190 K (b) with and without lightning occurrence. These data are used in the calculation of lightning probability in Figure 8. These are the gridded data for two northern and southern hemisphere summers that are combined into a summer database, namely Jul., Aug., and Sep. (JAS) of 2009 and 2010 for 0°-35° N and Jan., Feb., and Mar. (JFM) of 2010 and 2011 for 0°- 35° S (see Section 2 of paper). Note that the SSMIS sensor is on the DMSP F16 satellite that passes each location on earth two times per day at about 19:00 and 07:00 LST, and the TMI sensor on the TRMM satellite observes thunderstorms at various LSTs.

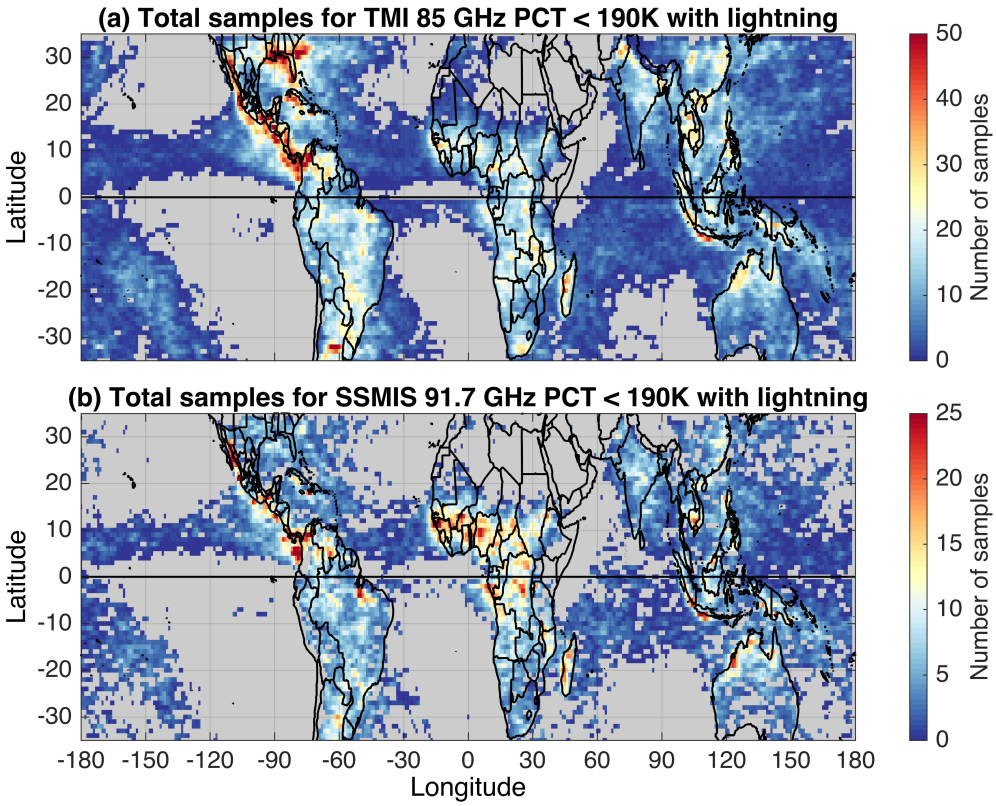

Figure S8. Total number of 0.5° × 0.5° grid square samples that satisfied TMI 85 GHz PCT < 190 K (a) and SSMIS 91.7 GHz < 190 K (b) with at least one lightning stroke. These data are used in the calculation of lightning probability in Figure 8. These are the gridded data for two northern and southern hemisphere summers that are combined into a summer database, namely Jul., Aug., and Sep. (JAS) of 2009 and 2010 for 0°-35° N and Jan., Feb., and Mar. (JFM) of 2010 and 2011 for 0°- 35° S (see Section 2 of paper). Note that the SSMIS sensor is on the DMSP F16 satellite that passes each location on earth two times per day at about 19:00 and 07:00 LST, and the TMI sensor on the TRMM satellite observes thunderstorms at various LSTs.

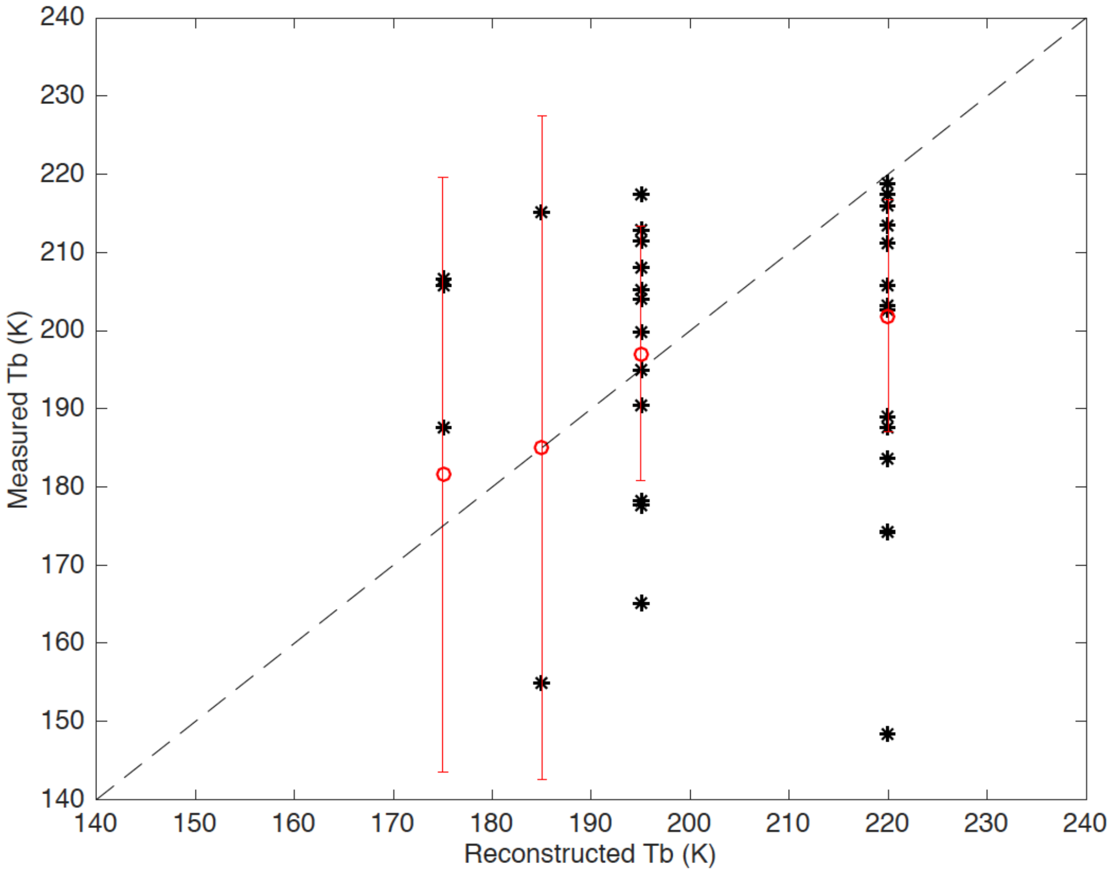

Figure S9. Reconstructed brightness temperatures using lightning rates vs. measured brightness temperatures by SSMIS 91.7 GHz PCT for the case study in Section 6 (Figure 13b). Black asterisk are the raw data, red circles are the mean of measured Tbs, and error bars are ±1 standard deviation of the measured Tbs. The dashed line shows measured Tb = reconstructed Tb. The correlation coefficient for the mean of measured Tbs vs. reconstructed Tbs is r=0.93. This should be interpreted cautiously as there are only four data points used here (due to binning the Tbs) and p=0.07.